LA-UR 07-4969
astro-ph/yymmnnn

arXiv:0709.1510v2 [astro-ph] 29 Sep 2007

The Most Dark Matter Dominated Galaxies: Predicted Gamma-ray Signals from the Faintest Milky Way Dwarfs

Louis E. Strigari,[1,*] Savvas M. Koushiappas,[2] James S. Bullock,[1]
Manoj Kaplinghat,[1] Joshua D. Simon,[3] Marla Geha,[4] and Beth Willman[5]

[1] *Center for Cosmology, Department of Physics and Astronomy, University of California, Irvine, CA 92697, USA*
[2] *Theoretical Division, & ISR Division, MS B227, Los Alamos National Laboratory, Los Alamos, NM 87545, USA*
[3] *Department of Astronomy, California Institute of Technology, 1200 E. California Blvd., MS105-24, Pasadena, CA 91125 USA*
[4] *National Research Council of Canada, Herzberg Institute of Astrophysics, 5071 West Saanich Road, Victoria, BC V9E, 2E7, Canada*
[5] *Harvard-Smithsonian Center for Astrophysics, 60 Garden St. Cambridge, MA, 02138*

(Dated: February 1, 2008)

We use kinematic data from three new, nearby, extremely low-luminosity Milky Way dwarf galaxies (Ursa Major II, Willman 1, and Coma Berenices) to constrain the properties of their dark matter halos, and from these make predictions for the γ-ray flux from annihilation of dark matter particles in these halos. We show that these $\sim 10^3$ $L_\odot$ dwarfs are the most dark matter dominated galaxies in the Universe, with total masses within 100 pc in excess of 10^6 $M_\odot$. Coupled with their relative proximity, their large masses imply that they should have mean γ-ray fluxes comparable to or greater than any other known satellite galaxy of the Milky Way. Our results are robust to both variations of the inner slope of the density profile and the effect of tidal interactions. The fluxes could be boosted by up to two orders of magnitude if we include the density enhancements caused by surviving dark matter substructure.

PACS numbers: 95.35.+d,14.80.Ly,98.35.Gi,98.62.Gq

I. INTRODUCTION

The census of the Local Group has changed dramatically in the last few years. Prior to the turn of the century, there were only eleven known satellite galaxies of the Milky Way (MW), with a discovery rate of roughly one new Local Group satellite per decade [1]. However, the Sloan Digital Sky Survey (SDSS) has been able to uncover a population of extremely low-luminosity satellite galaxies, which has roughly doubled the number of known satellites [2, 3, 4]. Determining how these new satellites fit in a given model for dark matter and cosmology presents a very exciting theoretical challenge.

The Cold Dark Matter (CDM) model predicts the existence of hundreds of MW satellites that are expected to host galaxies at the faint end of the luminosity function [5]. The ability of gas to cool and form stars in these low mass dark matter halos depends on a number of complex physical processes, such as supernova feedback, the photoionizing background, as well as mass loss due to tidal interactions [6]. Despite the broad range of observed luminosities, the dark matter masses for all of the pre-SDSS satellites are constrained to within relatively narrow range, approximately $\sim [1-6] \times 10^7$ $M_\odot$ within their inner 600 pc [7, 8]. Understanding this strong luminosity bias at the low mass end is crucial to deciphering the formation of these dwarf spheroidal (dSph) galaxies as well as to constraining the nature of dark matter.

In this paper we show that three new and nearby members of the Local Group discovered by the SDSS (Willman 1, Coma Berenices, and Ursa Major II) are likely to have masses comparable to their more luminous counterparts. Initial estimates have already shown that these galaxies have mass-to-light ratios similar to or larger than the pre-SDSS dwarfs [9, 10]. With luminosities more than two orders of magnitude less than the pre-SDSS dwarfs, these new satellites are not only interesting in the context of galaxy formation at the lowest-mass scales, but also for indirect dark matter detection. The new dwarfs are very faint, but they contain large amounts of dark matter and are located quite nearby, making them ideal sites to search for signals of dark matter annihilation.

Current and future observatories, including space-based experiments, such as GLAST [11], as well as a suite of ground-based Cerenkov detectors, such as STACEE [12], HESS [13], MAGIC [14], VERITAS [15], CANGAROO [16], & HAWK [17], will search for the signal of γ-rays from dark matter annihilations. The prospects for γ-ray detection from dark matter in well-known MW satellites with these observatories has been the subject of many previous studies [18, 19, 20]. All of these sys-

*Electronic address: lstrigar@uci.edu

tems are interesting targets not only because of their large mass-to-light ratios, but also because they are expected to have very low intrinsic γ-ray emission. This is in contrast to the situation at the Galactic center, where astrophysical backgrounds hinder the prospects of extracting the signal from dark matter annihilation [21]. Moreover, the known location of MW satellites makes a search of dark matter annihilation well-defined, unlike the search of completely dark substructure, which would rely on serendipitous discovery [22, 23, 24].

From the mass modeling of the dark matter halos, we provide the first determination of the γ-ray signal from dark matter from Ursa Major II, Willman 1, and Coma Berenices (Coma hereafter). These galaxies provide promising targets for γ-ray detection for three reasons: 1) they are the among the closest dark matter dominated systems, 2) they are expected to be free from intrinsic γ-ray emission, and 3) present data on their stellar kinematics suggest that their dark matter halos are as massive as the more well-known population of MW satellites.

This paper is organized as follows. In section II, we review the theoretical modeling of dwarf dark matter halos and the calculation of the γ-ray flux. In section III, we present the likelihood function for determining the flux, and outline the theoretical priors in the modeling. In sections IV and V we present the results and discussions.

II. THEORETICAL MODELING

When modeling the stellar distribution of a dwarf galaxy, it is important to determine the effect of external tidal forces on the dynamics of the system. For the MW satellites we study, we can obtain an estimate of the external tidal force by comparing its magnitude to the internal gravitational force. The internal gravitational force is $\sim \sigma^2/R$ and the external tidal force from the MW potential is $\sim (220\,\mathrm{km/s})^2 R/D^2$, where D is the distance to the dwarf from the center of the MW, and $220\,\mathrm{km/s}$ is the MW rotation speed at the distance of the dwarf. The MW satellites are characterized by scale radii of $R \sim 10-100$ pc and velocity dispersions $\sigma \sim 5-10$ km s^{-1}. For a typical distance of $D \sim 40$ kpc, the internal gravitational forces are thus larger by ~ 100.

An additional estimate of tidal effects can be obtained by comparing the internal crossing times of the stars in the galaxy to the orbital time scale of the system in the external potential of the host. For a galaxy with scale radii and velocity dispersions given above, an estimate of the crossing time is given by $R/\sigma \sim 1-20$ Myr. Assuming a rotation speed of ~ 220 km s^{-1} at the distance of these dSphs (~ 40 kpc), their orbital time scale in the MW potential is $\sim$ Gyr.

From the above estimates we conclude that *it is highly unlikely that these galaxies are presently undergoing significant tidal stripping.* These galaxies may have been tidally stripped before (for example, if their orbit took them closer to the center of the MW), however the stellar core that has survived is faithfully tracing the local potential [25, 26]. Of the galaxies we consider, only Ursa Major II shows strong evidence of past tidal interaction, as it is located on the same great circle as the Orphan Stream discovered by SDSS [3, 4]. Thus we can proceed ahead with confidence in modeling the surviving stellar cores as systems in dynamical equilibrium.

Line-of-sight velocities are widely used to determine the properties of the dark matter halos of dSphs [27, 28, 29] assuming spherical symmetry. For a system in dynamical equilibrium, the spherically symmetric Jeans equation gives the stellar line-of-sight velocity dispersion at a projected radius, R, from the center of the galaxy,

$$\sigma_t^2(R) = \frac{2}{I(R)}\int_R^\infty \left(1-\beta\frac{R^2}{r^2}\right)\frac{\rho_\star \sigma_r^2 r}{\sqrt{r^2-R^2}}dr, \quad (1)$$

where the three-dimensional velocity dispersion, σ_r is obtained from

$$r\frac{d(\rho_\star \sigma_r^2)}{dr} = -\rho_\star(r)V_c^2(r) - 2\beta(r)\rho_\star\sigma_r^2. \quad (2)$$

Here β is the stellar velocity anisotropy, and $\rho_\star(r)$ is the density profile for the stellar distribution, which is obtained from the projected stellar distribution, $I(R)$. The stellar distributions of the dSphs are typically fit with either Plummer or a King profiles [30]. The primary difference between these fits is that Plummer profiles are described by a single parameter, r_P, and fall-off as a power law in the outer regions of the galaxy, while King profiles are described by a core radius, r_K, and a cut-off radius, r_{cut}, and fall-off exponentially in the outer regions. For the stellar distributions of Ursa Major II and Coma, we use the Plummer fits compiled in [10], and for Willman 1 we use the King profile fit from [9]. These quantities, along with the distance to each galaxy and their respective luminosities, are given in Table I.

We model the distribution of dark matter in the dSphs with radial density profiles of the form

$$\rho(r) = \frac{\rho_s}{\tilde{r}^\gamma(1+\tilde{r})^{3-\gamma}}, \quad (3)$$

where ρ_s is the characteristic density, $\tilde{r} = r/r_s$, and r_s is the scale radius. Numerical simulations bound γ in the range $[0.7-1.2]$, and the outer slope is ~ -3 [31]. In order to compare the mass distribution in dSphs to dark matter halos in N-body simulations, it is useful to work in terms of the two parameters $V_{\max}$ and $r_{\max}$, the maximum circular velocity and the radius at which it is obtained. For example, for $\gamma = (0.8, 1, 1.2)$, $r_{\max}/r_s = (2.61, 2.16, 1.72)$. Thus, for a particular value of γ, the density profiles of dark matter halos can be described by either ρ_s-r_s or similarly by $V_{\max}$-$r_{\max}$.

With the parameters of the halo density profile specified, the γ-ray flux from dark matter annihilations is given by

$$\Phi = \frac{1}{2}P\int_0^{\xi_{max}} \sin\xi d\xi \int_{\eta_-}^{\eta_+}\left[\frac{\rho_s}{\tilde{r}^\gamma(1+\tilde{r})^{3-\gamma}}\right]^2 d\eta, \quad (4)$$

dSph	Distance (kpc)	Luminosity (10^3 L$_\odot$)	Core Radius (kpc)	Cut-off Radius (kpc)	Number of stars
Ursa Major II	32	2.8	0.127 (P)	—	20
Coma Berenices	44	2.6	0.064 (P)	—	59
Willman 1	38	0.9	0.02 (K)	0.08 (K)	47
Ursa Minor	66	290	0.30 (K)	1.50 (K)	187

TABLE I: The distance, luminosity, core and cut-off radii (Plummer (P), King (K)) for each of the dSphs we study. The last column gives the total number of stars used in the analysis.

where $\eta_\pm = D\cos\xi \pm \sqrt{r_t^2 - D^2\sin^2\xi}$, D is the distance to the galaxy, ξ is the angular distance from the center of the galaxy, and r_t is the tidal radius for the dark matter halo. Note that in the limit of $D \gg r_s$, the flux scales as $\int \rho(r)^2 dr/D^2$, and in the particular case where $\gamma = 1$, $\Phi \sim \rho_s^2 r_s^3/D^2$, with $\sim 90\%$ of the flux originating within r_s.

In Eq. (4), the properties of the dark matter particle are determined by

$$P = \frac{\langle\sigma v\rangle}{M_x^2}\int_{E_{\rm th}}^{M_\chi}\frac{dN}{dE}dE. \quad (5)$$

Here, $E_{\rm th}$ is a threshold energy, M_χ is the mass of the dark matter particle, $\langle\sigma v\rangle$ is the annihilation cross section, and the spectrum of the emitted γ-rays is given by dN/dE. Unless otherwise noted, we assume $P \approx 10^{-28}\mathrm{cm}^3\mathrm{s}^{-2}\mathrm{GeV}^{-2}$, which corresponds to the most optimistic supersymmetric dark matter models. However, we stress that the derived results can be rescaled to any dark matter model, by a simple rescaling of P.

III. LIKELIHOOD FUNCTION AND PRIORS

Observed stellar line-of-sight velocities place strong constraints on several important parameters describing the dark matter halos of dSphs. Two examples of these parameters are the halo mass and density at a characteristic halo radius, corresponding to about twice the King core radius (or about 600 pc for a typical dSph [7, 8]). More relevant to γ-rays is the quantity $\rho_s^2 r_s^3$ (the γ-ray luminosity is $\mathcal{L} \sim \rho_s^2 r_s^3$), which is typically determined to within a factor $3-6$ with the line-of-sight velocities of several hundred stars [19, 20]. The constraints on these parameters can be strengthened by including relations between similar parameters observed in numerical simulations. When combined with the observational constraints, these empirical relations in numerical simulations constitute a theoretical prior, delineating a preferred region of the parameter space of the dark matter distribution in dSphs [20, 32]. In this section, we discuss the implementation of this prior, and derive the general form of the likelihood function we use to constrain the γ-flux from dark matter annihilations.

We assume the line-of-sight velocities are drawn from a Gaussian distribution, centered on the true value of the mean velocity, u. This has been shown to be a good description of the well-studied dwarfs with line-of-sight velocities of several hundred stars [33]. Given the set of theoretical parameters, the probability to obtain the set of observed line-of-sight velocities, $\vec{\mathbf{x}}$, is

$$P(\vec{\mathbf{x}}|\vec{\theta}) = \prod_{i=1}^{n}\frac{1}{\sqrt{2\pi(\sigma_{t,\imath}^2+\sigma_{m,\imath}^2)}}\exp\left[-\frac{1}{2}\frac{(v_\imath - u)^2}{\sigma_{t,\imath}^2+\sigma_{m,\imath}^2}\right], \quad (6)$$

Here $\vec{\theta}$ is the set of parameters that describe the dSph, and the sum is over the observed total number of stars. The dispersion in the velocities thus has two sources: 1) the intrinsic dispersion, $\sigma_{t,\imath}(\vec{\theta})$, which is a function of the position of the $\imath^{th}$ star, and 2) the uncertainty stemming from the measurement, $\sigma_{m,\imath}$.

We can simplify Eq. (6) by assuming that the measurement uncertainties are small relative to the intrinsic dispersion. This is a good approximation for well-studied dwarfs, which have intrinsic dispersions $\sim 10\,\mathrm{km\,s^{-1}}$, and measurement errors $\sim 1\,\mathrm{km\,s^{-1}}$ [34]. Under this approximation Eq. (6) becomes

$$P(\vec{\mathbf{x}}|\vec{\theta}) = \prod_{\imath=1}^{N_B}\frac{1}{\sqrt{2\pi\sigma_{t,\imath}^2}}\exp\left[-\frac{1}{2}\frac{N_\imath\hat{\sigma}_{t,\imath}^2}{\sigma_{t,\imath}^2}\right], \quad (7)$$

where the sum is now over the number of bins, N_B, for which the velocity dispersion is determined. The velocity dispersion in the $\imath^{th}$ bin is $\hat{\sigma}_{t,\imath}^2$, and the number of stars in the $\imath^{th}$ bin is $N_\imath$. We can use Eq. (7) if the observations are given by line-of-sight velocity dispersions, and if the measurement errors are small in comparison to the intrinsic dispersion. This is the case for Ursa Minor, as discussed below.

We describe the dark matter halos in terms of the parameters $\vec{\theta} = (V_{\max}, r_{\max}, \beta)$. We assume that β is constant as a function of radius, and let it vary over the range $[-5:1]$. We integrate Eqs. (6) and (7) over these parameters and define the likelihood function for a fixed γ-ray flux, f, as

$$\begin{aligned}\mathcal{L}(f) \;&\propto\; \int P(\vec{\mathbf{x}}|V_{\max}, r_{\max}, \beta)P(V_{\max}, r_{\max}) \\ &\times\; \delta(\Phi(V_{\max}, r_{\max}) - f)dV_{\max}dr_{\max}d\beta. \quad (8)\end{aligned}$$

Here we have assumed a uniform prior on β, and the prior probability distribution for $V_{\max}, r_{\max}$ is given by

dSph	Mass < 100 pc [10^6 $M_\odot$]	$V_{\rm max}$ [km s^{-1}]
Ursa Major II	$3.1^{+5.6}_{-1.8}$	23^{+69}_{-10}
Coma Berenices	$1.9^{+2.1}_{-1.0}$	19^{+53}_{-9}
Willman 1	$1.3^{+1.5}_{-0.8}$	27_{-15}
Ursa Minor	$2.3^{+1.9}_{-1.2}$	30^{+12}_{-16}

TABLE II: The masses within 100 pc and the maximum circular velocities of the Milky Way satellites we study. Error bars indicate the 90% c.l. regions. No upper limit could be obtained for the maximum circular velocity of Willman 1.

$P(V_{\rm max}, r_{\rm max})$. This prior distribution is determined by the $V_{\rm max}$-$r_{\rm max}$ relation from CDM simulations.

In order to determine $P(V_{\rm max}, r_{\rm max})$, we need both its mean relation and its halo-to-halo scatter. For dark subhalos that have been strongly affected by tidal interactions, the $V_{\rm max} - r_{\rm max}$ relation is strongly dependent on the nature of the potential of the host system, as these systems undergo varying amounts of mass loss as they evolve within the host halo. For example, Bullock and Johnston [35] have embedded a disk potential in a MW size host halo, and found that the $V_{\rm max} - r_{\rm max}$ relation of subhalos takes the form $\log(r_{\rm max}) = 1.35[\log(V_{\rm max}) - 1] - 0.196$. We obtain a similar slope by examining the subhalos in the dark matter-only Via Lactea simulation of MW substructure [24], however differences in the assumed cosmological parameters, and the absence of a disk potential in Via Lactea, translate into differences in the normalization of the $V_{\rm max} - r_{\rm max}$ relation. For Via Lactea subhalos, we find the normalization is reduced by $\sim 30\%$, which implies reduced halo concentrations (larger $r_{\rm max}$ for fixed $V_{\rm max}$).

We model the scatter in $V_{\rm max}$ as a log-normal distribution, with $\sigma_{\log V_{\rm max}} \simeq 0.20$. This provides a conservative estimate for the scatter in $V_{\rm max}$ as a function of $r_{\rm max}$ for nearly the entire range of the subhalo mass function. At the extremely high end of the subhalo mass function ($V_{\rm max} \gtrsim 20\,{\rm km\,s^{-1}}$), the scatter increases because in this range it is dominated by a small number of very massive systems that have been accreted into the host halo very recently. This increase in the scatter is simply because Via Lactea is only one realization of a substructure population in a MW halo. We find that by excluding the extreme outliers in the Via Lactea mass function, the scatter is similar to the low mass regime. This is a similar result to those obtained in semi-analytic models of many realizations of the subhalo population [36, 37].

IV. RESULTS

A. Flux estimates for smooth dark matter distributions

We now quantify the prospects for detecting γ-rays from dark matter annihilation in the three new dSphs.

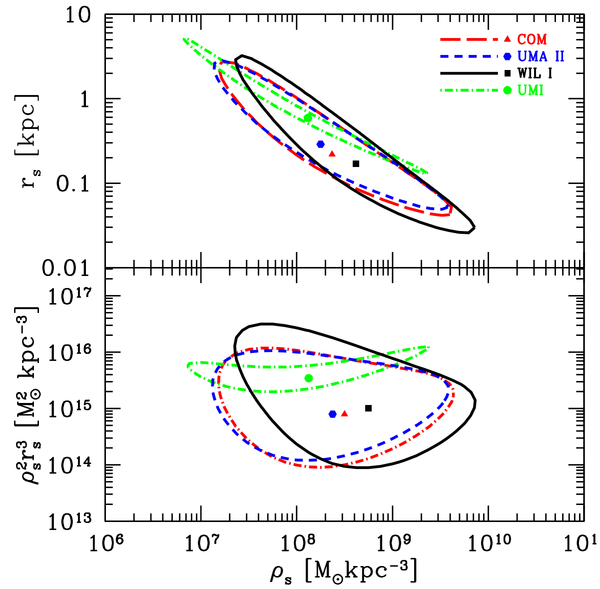

FIG. 1: The 90% confidence level region in the $\rho_s - r_s$ (top) $\rho_s^2 r_s^3 - \rho_s$ (bottom) parameter space for Coma , Ursa Major II, Willman 1, and Ursa Minor. We marginalize over the velocity anisotropy and have assumed an inner slope of $\gamma = 1$. The best-fit values are indicated with points.

We first assume that the dark matter is distributed smoothly, and we discuss the implications of a boost factor due to substructure in the next subsection. We use observations of these galaxies from the following references: Ursa Major II and Coma [10], Willman 1 [38]. For these galaxies we have individual stellar velocities, so we use the likelihood function in Eq. (6). To make a connection to previous studies of dSphs, we compare the fluxes for these new dSphs to the flux from Ursa Minor, which is at a distance $D = 66$ kpc, and has a luminosity of $L = 2.9 \times 10^5$ $L_\odot$. Ursa Minor has the largest flux of any of the well-known dwarfs [20]. We describe the stellar distribution of Ursa Minor with a King profile, with $r_K = 0.30$ kpc and $r_{cut} = 1.50$ kpc [39]. For Ursa Minor we use the measured velocity dispersion from a sample of 187 stars distributed evenly in 11 bins [39], and we use the likelihood function in Eq. (7).

In the top panel of Fig. (1), we show the 90% c.l. region in the $\rho_s - r_s$ plane for each galaxy, where the best-fit values are denoted by points. Here we use the $V_{\rm max} - r_{\rm max}$ prior from section III, and we take the inner slope of the dark matter halo profile to be $\gamma = 1$. In the bottom panel of Fig. (1) we show the 90% confidence level region in the $\rho_s^2 r_s^3 - \rho_s$ plane. As seen in Fig. (1), the range of values that $\rho_s^2 r_s^3$ can take in each dSph is reduced with the inclusion of more stars (e.g. Ursa Minor vs any one of the other three dSphs).

The constrained regions in Fig. (1) can be used to determine the masses, maximum circular velocities, and γ-ray flux probability distributions for each galaxy. In Ta-

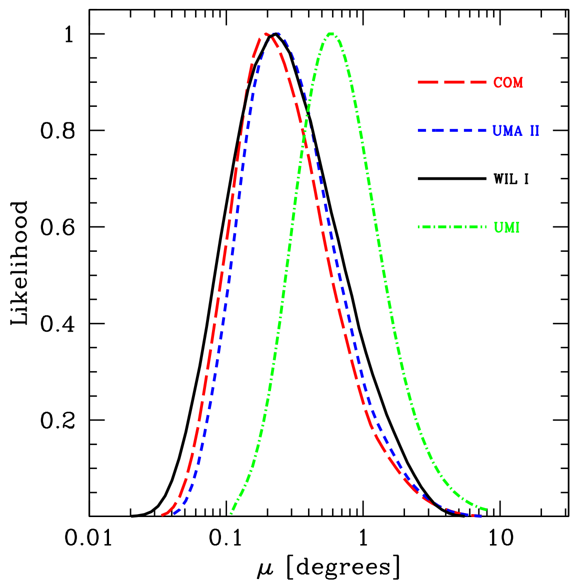

FIG. 2: The probability distributions of the angular size subtended by r_s for each galaxy. We marginalize over the velocity anisotropy and ρ_s. The inner slope is fixed to $\gamma = 1$.

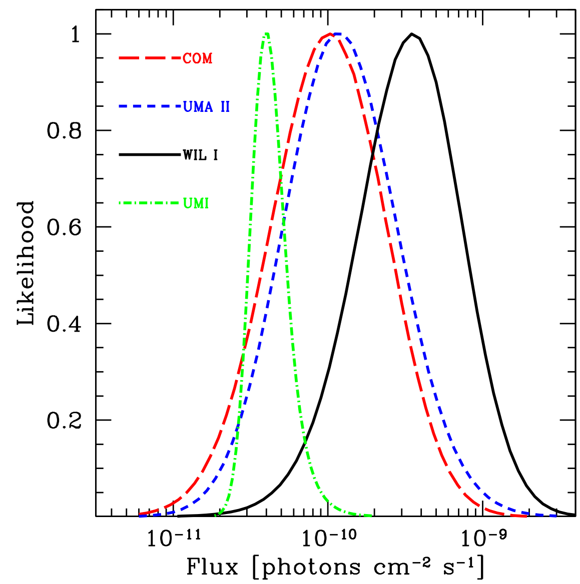

FIG. 3: The probability distributions for the γ-ray fluxes from Coma, Ursa Major II, Willman 1, and Ursa Minor, marginalizing over the velocity anisotropy, ρ_s, and r_s. We assume $P = 10^{-28}\,\mathrm{cm}^3\,\mathrm{s}^{-1}\,\mathrm{GeV}^{-2}$ and an inner slope of $\gamma = 1.0$. We have assumed no boost from halo substructure, which increases these fluxes by a factor $\sim 10 - 100$.

ble II, we show the masses within 100 pc and the maximum circular velocities for each galaxy. The error bars indicate the 90% c.l. regions.

To determine the flux distributions, we must first specify a solid angle for integration. For optimal detection scenarios, the solid angle should encompass the region with the largest signal-to-noise. For the present work, we will integrate over a region where 90% of the flux originates. As discussed above, for the particular case where $\gamma = 1$, 90% of the flux originates within r_s. Therefore, in order to estimate the solid angle of integration, we have to first determine the maximum likelihood values of r_s. This is done by marginalizing over ρ_s and β with the $V_{\rm max} - r_{\rm max}$ prior. The distributions of angular sizes are then obtained from $\mu = \tan^{-1}[r_s/D]$, where D is the distance to the dSph. As shown in Fig. (2), we find that given their similar size and roughly similar distances, all three dSphs will emit 90% of their $\gamma-$ray flux within a region of ~ 0.2 degrees, centered on each dSph (for $\gamma = 1$). Ursa Minor is the most physically extended galaxy, subtending the largest projected area on the sky.

It is important to determine whether each of the galaxies will be detected as point sources, or whether they will be resolved as extended objects. To determine this we compare their angular size to the angular resolution of γ-ray telescopes. GLAST will have a single photon angular resolution of ~ 10 arcminutes for energies greater than 1 GeV, similar to the angular resolution of ground-based detectors (such as VERITAS) for energies greater than few tens of GeV. In the case where the detected number of photons is $N_\gamma > 1$, the angular resolution of a detector is improved by a factor of $1/\sqrt{N_\gamma}$. Therefore, these galaxies can be resolved as extended objects, which in principle would allow a measured flux to determine the distribution of dark matter in the halo itself.

Fig. (3) depicts the resulting flux probability distribution for the three new dSphs and Ursa Minor. These are obtained by marginalizing over β, ρ_s, and r_s and including the $V_{\rm max}$-$r_{\rm max}$ prior. We set the inner slope to $\gamma = 1$, and integrate the flux over the solid angle that corresponds to 0.2 degrees from the center of the galaxy. We assume a value of $P = P_0 = 10^{-28}\mathrm{cm}^3\mathrm{s}^{-1}\,\mathrm{GeV}^{-2}$, but the result can be scaled to any dark matter candidate with a different value of P by simply multiplying the flux distribution by a factor of P/P_0.

The relative proximity of the three new dSphs, and their comparable sizes, results in γ-ray fluxes that are roughly similar. For $P \approx P_0$, the likelihood peaks at approximately $\Phi_0 \approx 10^{-10}\mathrm{cm}^{-2}\mathrm{s}^{-1}$, with a spread of nearly an order of magnitude. Thus Ursa Major II, Coma, and Ursa Minor all have comparable fluxes, and Willman 1 has a most likely flux that is about three times larger than Ursa Major II or Coma.

B. The effects of the inner slope and substructure boost factors

Understanding the distribution of dark matter in the inner regions of the dSphs also has important implications for detection of a γ-ray flux. However, when vary-

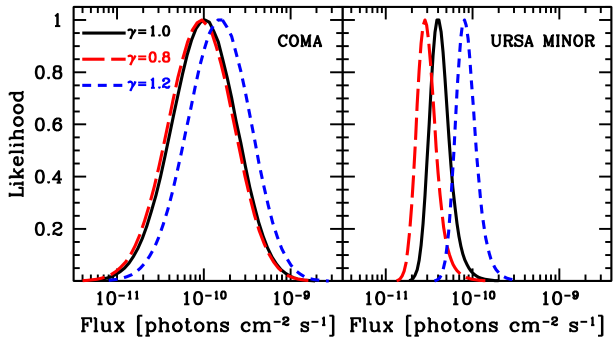

FIG. 4: The γ-ray flux probability distributions for Coma and Ursa Minor for inner slopes of 0.8 (long-dashed), 1.0 (solid), and 1.2 (short-dashed). We marginalize over the same quantities as in Fig. (3). The value of P is the same as in Fig. (3).

ing the inner slope, we must also be certain to vary all of the other halo parameters so as to remain consistent with the line-of-sight observations. In order to quantify the effects of varying the inner slope, we marginalize over $V_{\rm max}$, $r_{\rm max}$ and β for profiles with different values of γ. In Fig. (4) we show the effects of varying γ for Coma and Ursa Minor. The shifts in the flux distribution function are not only a result of varying the inner slope but also come from the constraints imposed by the data on the density profile parameters ρ_s and r_s. The relative amount of the shifts can be understood by considering the best-fitting values of r_s (where the majority of the γ-ray flux comes from) as compared to the core radii of the systems. When the core radius is similar to r_s, the shifts are larger for varying γ, as in the case of Ursa Minor. However, when the core radius is much smaller than the fitted values of r_s, variations in the inner slope are less significant than the change induced by ρ_s, as is the case for Coma.

The presence of substructure in dark matter halos is firmly established on theoretical and numerical grounds. Dark matter halos are approximately self-similar, and substructure is expected to be present in all dark matter halos with mass greater than the cut-off scale in the primordial power spectrum, set by the kinetic decoupling temperature of the dark matter particle (for detecting the smallest dark matter halos in the Milky Way, see [23]). It is therefore natural to expect that these galaxies contain substructure if they consist of CDM.

The density enhancement over the smooth distribution of dark matter leads to an enhancement in the total annihilation rate, typically quantified in terms of a "boost" factor. As was shown in [20], the boost factor cannot attain arbitrarily large values, but instead is bounded to be less than ~ 100, with the exact value depending on the cut-off scale in the CDM mass function. The boost is a multiplicative quantity, so the effect of dark substructure is simply accounted for by scaling the fluxes in Fig. (3) by the appropriate boost factor.

C. Detection prospects

As is shown in Fig. (3), the flux probability distribution functions peak around $\Phi_0 \approx 10^{-10}\mathrm{cm}^{-2}\mathrm{s}^{-1}$ without including any enhancement to the signal from substructure. Here, we will assume a conservative value of 10 for the boost factor, and discuss the prospects for detecting the three new dSphs with γ-ray instruments. We can make simple estimates for the likelihood for detection by adopting the specifications of particular γ-ray detectors. We will use two examples: a space-based experiment, GLAST, and a ground-based Cerenkov telescope, VERITAS. For GLAST, if we assume an orbit-averaged effective area of $A_{\rm eff} \approx 2\times10^3\mathrm{cm}^2$ and an exposure time of $t_{\rm exp} = 10$ years, their product is $B_{\rm G} = A_{\rm eff} t_{\rm exp} \approx 3\times10^{11}\mathrm{cm}^2\mathrm{s}$. A 50 hour exposure with VERITAS ($A_{\rm eff} \approx 10^8\mathrm{cm}^2$) has $B_{\rm V} \approx 2\times10^{13}\mathrm{cm}^2\mathrm{s}$. Naively, for a fixed value of P, a ground-based detector seems more sensitive because $B_{\rm V} > B_{\rm G}$. However, the backgrounds for a ground-based detector are also larger and include a component from the hadronization of cosmic rays in the atmosphere.

As an example, for a fixed value of $P = P_0$, and a solid angle that corresponds to an angular size of 0.2 degrees, the number of photons detected by GLAST is $N_{\gamma,G} \approx 300$. The dominant source of background for GLAST is the Galactic diffuse emission ($dN_B/dE = 1.2\times10^{-6}[E_{\rm th}/\,\mathrm{GeV}]^{-1.1}\mathrm{cm}^{-2}\mathrm{s}^{-1}\mathrm{sr}^{-1}\,\mathrm{GeV}^{-1}$ [40]). If we assume an energy threshold of $E_{\rm th} \approx 1\,\mathrm{GeV}$, then the number of background photons is $N_B = B_{\rm G}\, dN_B/dE \approx 250$, which means that the new satellites will be detected at approximately a $N_{\gamma,G}/\sqrt{N_B + N_{\gamma,G}} \approx 12\sigma$ level. A similar estimate can be obtained for VERITAS. The number of photons detected above 50 GeV in an instrument with an effective area times exposure $\sim B_{\rm V}$ is $N_\gamma \approx 2\times10^4$. The dominant contribution to the background are photons that originate from neutral pion decays from the nuclear interactions of cosmic rays in the upper layers of the atmosphere ($dN_B/dE = 3.8\times10^{-3}[E_{\rm th}/\,\mathrm{GeV}]^{-2.75}\mathrm{cm}^{-2}\mathrm{s}^{-1}\mathrm{sr}^{-1}\,\mathrm{GeV}^{-1}$ [41]). The number of background photons from pion decays is approximately $N_B \approx 2\times10^7$, therefore the 3 dSphs could be detected at a $\nu \approx 5\sigma$ level. Understanding and discriminating against the background contamination in Cerenkov telescopes is very important in improving the prospects for detecting dSphs of the Milky Way.

As shown in [20], the large number of stellar velocities obtained in the older dSphs allow useful γ-ray flux ratios between different dSphs to be determined. For the three new dSphs considered in this work, the kinematic data is not good enough to play the same game. Clearly, more stellar velocities will shrink the allowed region of $\rho_s^2 r_s^3$ parameter permitting robust estimates of flux ratios between the galaxies studied here and the rest of the Milky Way satellites.

V. DISCUSSION & CONCLUSIONS

In this paper, we have modeled the dark matter distribution in three recently-discovered Milky Way (MW) satellites (Ursa Major II, Willman 1, and Coma Berenices), and have presented the prospects for detecting γ-rays from dark matter annihilations in their halos. We show that the expected flux from these galaxies is larger than the flux from any of the higher luminosity, more well-known (pre-SDSS) dwarfs. There are two reasons for this surprising result: 1) the masses of these new dwarfs within their stellar distributions are similar to the masses of the well-known, larger luminosity dwarfs, and 2) all three new galaxies are closer than the other well-known dwarfs. The implied mass-to-light ratios, ~ 1000, of these new dwarfs makes them the most dark matter dominated galaxies in the Universe.

Our estimates show that it is unlikely that the observed stellar distributions are presently undergoing tidal disruption. However, this does not mean that they have been free from tidal interactions in the past, but rather that the surviving stellar core can be faithfully modeled as a system in dynamical equilibrium. By including the $V_{\rm max} - r_{\rm max}$ CDM prior, we have naturally accounted for tidal effects in the mass modeling, since this $V_{\rm max} - r_{\rm max}$ relation in fact comes from dark matter halos that have experienced tidal stripping.

One of the galaxies we consider, Ursa Major II, may be a candidate for past tidal disruption, given that it is positioned on the same great circle as the Orphan Stream of stars, which was also recently detected by the SDSS [3, 4]. This is consistent with the findings of Simon and Geha [10], who have recently investigated the possibility of tidal disruption in Ursa Major II, as well as all of the other new dwarfs, using proxies such as gradients in the observed velocity distribution and metallicity of the stellar populations. Given the total mass-to-light ratio we have determined for Ursa Major II, tidal stripping will have only been significant if its pericenter is $\sim$ 3 times closer than its present distance. Future observations of the stellar distributions in Ursa Major II, and all of the other new faint dwarfs, will be important in determining bound and unbound stellar populations. With a larger sample of stars from a galaxy such as Ursa Major II, it will be possible to remove unbound and interloping stars with techniques similar to those presented in [25]. Upon removal of stars unbound to the galaxy, these authors show that in most cases the true bound mass of the system can be recovered to typically better than 25%.

As a very conservative check for the effects of membership uncertainties, we have redone the analysis for each of the galaxies by just keeping the stars within the inner half of each galaxy, where the surface densities are the most well-determined. We find that the peak of the flux likelihood is shifted by a small amount relative to the 1-σ widths in Fig. (3). Note however, that even when including the entire population of stars in the observed samples, in all cases equilibrium models provide adequate descriptions of the dynamics of each system.

Unresolved binary star systems also introduce a systematic that may effect the fluxes we have presented. Olszewski, Pryor, and Armandroff [42] have determined the effect of binaries on the velocity dispersion of two of the most luminous dwarfs, Draco and Ursa Minor, by inferring the binary population of these systems using multiple epoch observations. They find a velocity dispersion of $\sim 1.5\,{\rm km\,s^{-1}}$ due to binaries, and a probability of 5% that binaries elevate the velocity dispersion to $4\,{\rm km\,s^{-1}}$, which is still less than the velocity dispersion of the three new dwarfs. Thus if Ursa Major II, Willman 1, and Coma have binary fractions similar to Draco and Ursa Minor, their observed velocity dispersions are not significantly affected by binaries. We note that this is consistent with recent estimates of the binary fraction in low density Galactic globular clusters [43].

A strong test for the presence of binaries is to examine the distribution of measured velocities. The velocity distribution due to internal motion in binary systems should be flat due to the observed broadness of the period distribution of binaries [44]. The observed period distributions depend on spectral type and age of the system (among other variables) but are all broad with dispersions of about two orders of magnitude, which seems to be consistent with theoretical expectations [45]. Further, there is no observational evidence or theoretical argument that suggests that the period distribution should be sharply suppressed for all periods below $\sim$ 1000 years (roughly velocities larger than $\sim$ 3 km/s). Thus if there is a large contribution from internal motion in binary stellar systems to the intrinsic velocity dispersion of these dwarfs, we expect to see a significant tail of high velocities. This is not observed and hence we can be confident that measured velocity dispersion is tracing the total mass in the dwarf galaxy.

The new, ultra-low luminosity galaxies represent an interesting confluence of astronomical and γ-ray studies. Future kinematic studies of all of these new dwarfs will further reduce the errors on the mass distributions, and sharpen the predictions for γ-ray observatories searching for signatures of dark matter annihilations.

VI. ACKNOWLEDGMENTS

We are grateful to Simon White for many useful discussions on likelihood functions for dwarf galaxies; Jay Strader and Connie Rockosi for Willman 1 data; Juerg Diemand, Michael Kuhlen, and Piero Madau for making the data from the Via Lactea simulation publicly available; and John Beacom, Nicolas Martin, and Joe Wolf for useful discussions. JSB, LES, and MK are supported in part by NSF grant AST-0607746. Work at LANL was carried out under the auspices of the NNSA of the U.S. Department of Energy at Los Alamos National Laboratory under Contract No. DE-AV52-06NA25396. JDS gratefully acknowledges the support of a Millikan Fellow-

ship provided by Caltech.

---

[1] M. Mateo, Ann. Rev. Astron. Astrophys. **36**, 435 (1998) [arXiv:astro-ph/9810070].

[2] B. Willman *et al.*, Astrophys. J. **626**, L85 (2005) [arXiv:astro-ph/0503552]; M. J. Irwin *et al.*, Astrophys. J. **656**, L13 (2007) [arXiv:astro-ph/0701154]; S. M. Walsh, H. Jerjen and B. Willman, arXiv:0705.1378 [astro-ph].

[3] D. B. Zucker *et al.*, Astrophys. J. **650**, L41 (2006) [arXiv:astro-ph/0606633].

[4] V. Belokurov *et al.* [SDSS Collaboration], Astrophys. J. **654**, 897 (2007) [arXiv:astro-ph/0608448].

[5] G. Kauffmann, S. D. M. White and B. Guiderdoni, Mon. Not. Roy. Astron. Soc. **264** (1993) 201. A. A. Klypin, A. V. Kravtsov, O. Valenzuela and F. Prada, Astrophys. J. **522**, 82 (1999) [arXiv:astro-ph/9901240]. B. Moore, S. Ghigna, F. Governato, G. Lake, T. Quinn, J. Stadel and P. Tozzi, Astrophys. J. **524**, L19 (1999).

[6] J. S. Bullock, A. V. Kravtsov and D. H. Weinberg, Astrophys. J. **539**, 517 (2000) [arXiv:astro-ph/0002214]; W. A. Chiu, N. Y. Gnedin, and J. P. Ostriker, Astrophys. J. **563**, 21 (2001) [astro-ph/0103359]; A. J. Benson, C. G. Lacey, C. M. Baugh, S. Cole and C. S. Frenk, Mon. Not. Roy. Astron. Soc. **333**, 156 (2002) [arXiv:astro-ph/0108217]; R. Barkana and A. Loeb, Astrophys. J. **523**, 54 (1999) [arXiv:astro-ph/9901114]; A. Dekel and J. Silk, Astrophys. J. **303**, 38 (1986); S. Cole, A. Aragon-Salamanca, C. S. Frenk, J. F. Navarro and S. E. Zepf, Mon. Not. Roy. Astron. Soc. **271**, 781 (1994) [arXiv:astro-ph/9402001]; R. S. Somerville and J. R. Primack, Mon. Not. Roy. Astron. Soc. **310**, 1087 (1999) [arXiv:astro-ph/9802268].

[7] M. G. Walker, M. Mateo, E. W. Olszewski, O. Y. Gnedin, X. Wang, B. Sen and M. Woodroofe, arXiv:0708.0010 [astro-ph].

[8] L. E. Strigari, J. S. Bullock, M. Kaplinghat, J. Diemand, M. Kuhlen and P. Madau, arXiv:0704.1817 [astro-ph].

[9] N. F. Martin, R. A. Ibata, S. C. Chapman, M. Irwin and G. F. Lewis, arXiv:0705.4622 [astro-ph].

[10] J. D. Simon and M. Geha, Astrophys. J. in press, arXiv:0706.0516 [astro-ph].

[11] S. Ritz., J. Grindlay, C. Meegan, P. F. Michelson, & GLAST Mission Team 2005, Bulletin of the American Astronomical Society, 37, 1198.

[12] D. S. Hanna *et al.*, Nucl. Instrum. Meth. A **491**, 126 (2002) [arXiv:astro-ph/0205510].

[13] W. Hofmann [HESS Collaboration], *Prepared for 28th International Cosmic Ray Conferences (ICRC 2003), Tsukuba, Japan, 31 Jul - 7 Aug 2003.*

[14] J. Cortina *et al.* [MAGIC Collaboration], *Prepared for 29th International Cosmic Ray Conference (ICRC 2005), Pune, India, 3-11 Aug 2005*

[15] T. C. Weekes *et al.*, Astropart. Phys. **17**, 221 (2002) [arXiv:astro-ph/0108478].

[16] T. Yoshikoshi *et al.*, Astropart. Phys. **11**, 267 (1999).

[17] G. Sinnis [HAWC Collaboration], AIP Conf. Proc. **745** (2005) 234.

[18] E. A. Baltz, C. Briot, P. Salati, R. Taillet and J. Silk, Phys. Rev. D **61**, 023514 (2000) [arXiv:astro-ph/9909112]; N. W. Evans, F. Ferrer and S. Sarkar, Phys. Rev. D **69**, 123501 (2004) [arXiv:astro-ph/0311145]; S. Profumo and M. Kamionkowski, JCAP **0603**, 003 (2006) [arXiv:astro-ph/0601249]; M. A. Sanchez-Conde, F. Prada, E. L. Lokas, M. E. Gomez, R. Wojtak and M. Moles, arXiv:astro-ph/0701426.

[19] L. Bergstrom and D. Hooper, Phys. Rev. D **73**, 063510 (2006) [arXiv:hep-ph/0512317].

[20] L. E. Strigari, S. M. Koushiappas, J. S. Bullock and M. Kaplinghat, Phys. Rev. D **75**, 083526 (2007) [arXiv:astro-ph/0611925].

[21] D. Hooper and B. L. Dingus, Phys. Rev. D **70**, 113007 (2004) [arXiv:astro-ph/0210617].

[22] C. Calcaneo-Roldan and B. Moore, Phys. Rev. D **62**, 123005 (2000) [arXiv:astro-ph/0010056]; A. Tasitsiomi and A. V. Olinto, Phys. Rev. D **66**, 083006 (2002) [arXiv:astro-ph/0206040]; F. Stoehr, S. D. M. White, V. Springel, G. Tormen and N. Yoshida, Mon. Not. Roy. Astron. Soc. **345**, 1313 (2003) [arXiv:astro-ph/0307026]; S. M. Koushiappas, A. R. Zentner and T. P. Walker, Phys. Rev. D **69**, 043501 (2004) [arXiv:astro-ph/0309464]; E. A. Baltz, J. E. Taylor and L. L. Wai, arXiv:astro-ph/0610731; L. Pieri, E. Branchini and S. Hofmann, Phys. Rev. Lett. **95**, 211301 (2005) [arXiv:astro-ph/0505356];

[23] S. M. Koushiappas, Phys. Rev. Lett. **97**, 191301 (2006) [arXiv:astro-ph/0606208].

[24] J. Diemand, M. Kuhlen and P. Madau, Astrophys. J. **657**, 262 (2007) [arXiv:astro-ph/0611370].

[25] S. Piatek and C. Pryor, Astron. J. **109**, 1071 (1995); J. Klimentowski, E. L. Lokas, S. Kazantzidis, F. Prada, L. Mayer and G. A. Mamon, Mon. Not. Roy. Astron. Soc. **378**, 353 (2007) [arXiv:astro-ph/0611296].

[26] J. Penarrubia, J. F. Navarro and A. W. McConnachie, arXiv:0708.3087 [astro-ph].

[27] E. L. Lokas, G. A. Mamon and F. Prada, Mon. Not. Roy. Astron. Soc. **363**, 918 (2005) [arXiv:astro-ph/0411694].

[28] S. Mashchenko, A. Sills and H. M. P. Couchman, Astrophys. J. **640**, 252 (2006) [arXiv:astro-ph/0511567].

[29] G. Gilmore, M. I. Wilkinson, R. F. G. Wyse, J. T. Kleyna, A. Koch, N. W. Evans and E. K. Grebel, arXiv:astro-ph/0703308.

[30] I. King, Astron. J. **67**, 471 (1962).

[31] J. F. Navarro *et al.*, Mon. Not. Roy. Astron. Soc. **349**, 1039 (2004) [arXiv:astro-ph/0311231]; J. Diemand, M. Zemp, B. Moore, J. Stadel and M. Carollo, Mon. Not. Roy. Astron. Soc. **364**, 665 (2005) [arXiv:astro-ph/0504215].

[32] J. Penarrubia, A. McConnachie and J. F. Navarro, arXiv:astro-ph/0701780.

[33] M. G. Walker, M. Mateo, E. W. Olszewski, , R. Bernstein, X. Wang, & M. Woodroofe, Astron. J. , **131** 2114 (2006) [arXiv:astro-ph/0511465].

[34] K. B. Westfall *et al*, Astron. J. , **131** 375 (2006) [arXiv:astro-ph/0508091]; A. Koch *et al.*, Astrophys. J. **657**, 241 (2007) [arXiv:astro-ph/0611372].

[35] J. S. Bullock and K. V. Johnston, Island Universes, As-

trophysics and Space Science Proceedings Springer, 227 (2007).
[36] A. R. Zentner and J. S. Bullock, Astrophys. J. **598**, 49 (2003) [arXiv:astro-ph/0304292].
[37] F. C. van den Bosch, G. Tormen and C. Giocoli, Mon. Not. Roy. Astron. Soc. **359**, 1029 (2005) [arXiv:astro-ph/0409201].
[38] B. Willman, M. Geha, J. Strader, and C. Rockosi in preparation.
[39] R. R. Munoz *et al.*, Astrophys. J. **631**, L137 (2005) [arXiv:astro-ph/0504035].
[40] S. D. Hunter *et al.*, Astrophys. J. **481**, 205 (1997).
[41] J. Nishimura *et al.*, Astrophys. J. **238**, 394 (1980).
[42] E. Olszewski, C. Pryor and T. Armandroff, Astron. J. **111**, 750 (1996) [arXiv:astro-ph/9510155].
[43] A. Sollima, G. Beccari, F. R. Ferraro, F. Fusi Pecci and A. Sarajedini, arXiv:0706.2288 [astro-ph].
[44] A. Duquennoy and M. Mayor, Astron. Astrophys. **248**, 485 (1991).
[45] R. T. Fisher, Astrophys. J. **600**, 769 (2004) [arXiv:astro-ph/0303280].